Acta Cryst. (1990). B46, 390–399

Neutron Diffraction Study of the Structure II Clathrate Hydrate: $3{\cdot}5Xe.8CCl_4.136D_2O$ at 13 and 100 K*

BY R. K. MCMULLAN AND Å. KVICK

Chemistry Department, Brookhaven National Laboratory, Upton, NY 11973, *USA*

(*Received* 20 *October* 1989; *accepted* 17 *November* 1989)

In memory of Dr D. W. Davidson

Abstract

The crystal structure of the clathrate hydrate, $3{\cdot}5Xe.8CCl_4.136D_2O$, at 13 and 100 K has been determined from single-crystal neutron diffraction data. The crystals are cubic, space group $Fd3m$, with $a_0 = 17{\cdot}192$ (1) Å at 13 K and 17·240 (2) Å at 100 K. The structure was refined by least-squares methods with expansion coefficients of spherical harmonics as parameters describing rotational disorder of the CCl_4 molecules. The $wR(F^2)$ indices are 0·040, 0·039 (13, 100 K) for 524, 522 reflections and 64, 61 parameters. The D_2O molecules are disordered at 13 and 100 K in six hydrogen-bonded orientations of equal statistical weights, as in ice I*h*. There are six non-equivalent hydrogen-bond interactions with O···D distances (at 13 K) between 1·738 (3) and 1·802 (1) Å and O···D—O angles between 174·8 (1) and 180°. The covalent O—D lengths (uncorrected for thermal motion) are in the range 0·986 (1)–1·001 (2) Å and are decreased significantly from 13 to 100 K. The Xe atoms occupy statistically 22% of the dodecahedra and vibrate about the cage centers with r.m.s. displacements of 0·137 Å at 13 K and 0·179 Å at 100 K. The CCl_4 molecules exhibit large-amplitude libration motion about the C atom located at the center of the hexakaidecahedron. There are seven preferred molecular orientations with C—Cl bonds directed toward the O vertices of the $(D_2O)_{28}$ polyhedron. The C—Cl bond length from the radius parameter of the spherical distribution is 1·765 (2) Å at 13 K and 1·762 (3) Å at 100 K, compared with the gas-phase value of 1·766 (3) Å.

Introduction

The crystal structure of the clathrate hydrate, $3{\cdot}5Xe.8CCl_4.136D_2O$ (Waller, 1960), has been determined by neutron diffraction in order to study the distribution of deuterium atoms and guest Xe and CCl_4 molecules in the water host structure of type II that characterizes one major group of gas hydrates (von Stackelberg & Müller, 1954). The structural relationships among clathrate hydrates have recently been reviewed by Jeffrey (1984). X-ray diffraction data at 255 K on the structure II clathrate, $7{\cdot}33H_2S.8C_4H_8O.136H_2O$ (Mak & McMullan, 1965), give precise positions for water oxygen atoms but do not describe conclusively the molecular orientations or proton ordering in the hydrogen-bonded water framework. As in this case, the guest configurations within clathrate structures often cannot be defined precisely from diffraction data: the guests of low molecular symmetry are statistically disordered with freedom to reorient within highly symmetrical water environments. In the clathrate selected for this study, the CCl_4 guest has the symmetry of its crystal site, T_d, and static orientational disorder is thus not a crystallographic requirement. The CCl_4 clathrate crystals appear to form only in the presence of *help gases* such as Xe which fill smaller voids in the water framework and stabilize the structure (von Stackelberg & Frühbuss, 1954). Xenon gas is reported to be especially effective in this role (Waller, 1960), and we have found that the *double hydrate* crystals formed in its presence are of good quality for single-crystal neutron studies. The crystal structure has been determined at two low temperatures, 13 and 100 K. The purpose of the temperature-dependent measurements was to aid our efforts to understand the dynamic and static disorder in the structure.

Experimental

The clathrate compound was prepared from a degassed mixture of CCl_4 and D_2O in the mole ratio 1:17 under Xe gas at 1 atm. The crystalline powder formed on cooling slowly sublimed and recrystallized at 278 K yielding large hexagonal plates with prominent forms {110} and {111}. The crystal selected for study (Table 1) was affixed to an aluminium pin at 213 K and sealed under He gas inside an aluminium canister.

* Research carried out at Brookhaven National Laboratory under contract DE-AC02-76CH00016 with the US Department of Energy and supported by its Office of Basic Energy Sciences.

0108-7681/90/030390-10$03.00

Table 1. *Summary of diffraction measurements and structure refinements on* $3{\cdot}5Xe.8CCl_4.136D_2O$

The $3{\cdot}5Xe.8CCl_4.136D_2O$ composition is from the structure refinement.

Crystal sample				
Principal faces		{110}, {111}		
Dimensions (mm)		2·0 × 2·4 × 1·7		
Volume (mm³)		6·1		
Absorption coefficient,[a] μ (cm^{-1})		0·403		
Crystal data		13 K	100 K	
Space group		*Fd3m*	*Fd3m*	
Lattice constant (Å)		17·192 (1)	17·240 (2)	
Cell volume (Å³)		5081·4 (8)	5124·0 (17)	
Density (g cm^{-3})		1·44 (2)	1·43 (2)	
Diffraction measurements				
Temperature (K)		13·0 (5)	100·0 (5)	
Wavelength (Å)		1·0470 (1)	1·0470 (1)	
Sinθ/λ limit (Å^{-1})		0·78	0·78	
Number of observations				
Total		1074	1065	
Independent, n		524	522	
Internal agreement[b]		0·023	0·024	
Refinement	1[c]	2[d]	1[c]	2[d]
Number of variables, v	66	64	66	61
Scale factor, k	1·457 (3)	1·459 (3)	1·453 (3)	1·455 (3)
Extinction parameter,[e] g	2·3 (5)	2·0 (5)	2·9 (5)	2·8 (5)
Indices of fit[f]				
$R(F^2)$	0·041	0·041	0·049	0·047
$wR(F^2)$	0·041	0·040	0·040	0·039
S	1·043	1·142	1·016	0·988

Notes: (*a*) Evaluated from μ/ρ (*International Tables X-ray Crystallography*, 1962, p. 197). (*b*) $\sum w|F_i^2 - \bar{F}^2|/\sum w\bar{F}^2$ from equivalent F_i^2 values with weights w from counting statistics. (*c*) Conventional independent-atom refinement: thermal parameters U_{ij} for all atoms: Cl atoms disordered over three non-equivalent sites (see Table 2). (*d*) Rigid-body refinement of CCl_4: Cl-scattering density by symmetry-adapted spherical harmonics; otherwise as in (*c*). (*e*) Isotropic $g \times 10^3$ rad^{-1} for type-I crystal with Lorentzian mosaic distribution. (*f*) $R(F^2) = \sum|F_o^2 - F_c^2|^2/\sum F_o^2$; $wR(F^2) = [\sum w|F_o^2 - F_c^2|^2/\sum(wF_o^2)^2]^{1/2}$; $S = [\sum w|F_o^2 - F_c^2|^2/(n-v)]^{1/2}$.

The diffraction data were measured on a four-circle diffractometer at the Brookhaven High Flux Beam Reactor. The neutron beam, monochromatized by reflection from the 002 planes of a Be crystal, was of wavelength 1·0470 (1) Å based on a prior calibration with a KBr crystal ($a_0 = 6{\cdot}6000$ Å at 298 K). The temperature of the sample crystal was maintained with a closed-cycle helium refrigerator* within 0·5° of preset values.† Measurements were made first at 13 K and then at 100 K. The diffraction symmetry $m3m$ and extinction rules for space group $Fd3m$ were verified from intensity data on equivalent reflections measured at 13 K. The lattice periodicity of ~17 Å was confirmed by $\omega/2\theta$ scans along the principal crystal directions at 13 K. Precise values of a_0 were determined by least-squares fits of $\sin^2\theta$ values for 32 reflections distributed over the lattice in the range $42 < 2\theta < 52°$. Intensity data for reflections with $\sin\theta/\lambda < 0{\cdot}78$ Å^{-1} were collected in two equivalent sectors ($h \le k \le l$ and $h \le l \le k$) by the $\omega/2\theta$ step-scan method. The scan ranges in $\Delta 2\theta$ were fixed at 3·0° for $0 < 2\theta < 50°$ and were varied as $\Delta 2\theta = (2{\cdot}92 + 2{\cdot}19\tan\theta)°$ for $50 < 2\theta < 109°$. Intervals between steps were adjusted to give 65 to 85 points in the scans. Counts were accummulated at each point for a preset monitor count of the incident beam, which required ~2 s. The intensities of two reflections (0,10,10 and 10,0,$\bar{1}$0) were remeasured at ~3 h intervals and were found to be constant within 2%. The integrated intensity I for each reflection was obtained by subtracting the background B as estimated from the two outer 10% parts of the scan. The variance $\sigma^2(I)$ was derived from counting statistics. The intensity data were corrected for absorption by an analytical procedure (de Meulenaer & Tompa, 1965; Templeton & Templeton, 1973), using measured crystal dimensions and $\mu = 0{\cdot}403$ cm^{-1}. Transmission factors ranged between 0·928 and 0·938 or about 1% for a crystal of the size used. Symmetry-related F^2 ($= I\sin 2\theta$) values were averaged in each data set to give the independent observations (524 at 13 K, 522 at 100 K) used in the structure determination. Additional numerical details are given in Table 1.

* Air Products and Chemicals, Inc., Displex Model CS-202.

† The reported temperatures are based on a prior calibration with reference to the magnetic phase transition in FeF_2 at 78·4 K (Hutchings, Schulhof & Guggenheim, 1972).

Refinement

Initial positions for the D_2O molecules were taken from the X-ray structure determination of $7{\cdot}33H_2S.8C_4H_8O.136H_2O$ (Mak & McMullan, 1965) and were readjusted by Fourier methods using the 13 K data. The Xe and CCl_4 molecules were located in difference maps inside the smaller and larger types of cages, respectively, of the host structure. The Cl-scattering density occurred as diffuse peaks on a spherical shell of low density. These peaks defined three non-equivalent orientations for the CCl_4 molecule. Trial population parameters for the CCl_4 configurations were derived from relative heights of the Cl peaks assuming full occupancy of the cage by CCl_4 in three distinct orientations. The complete structure model is symmetry-generated from equivalent positions of $Fd3m$ given in Table 2. The parameters of the alternative CCl_4 models labelled 'discrete atom' and 'rotator' were in turn varied with the positional and anisotropic thermal parameters of O, D, Xe and C in refinements against both data sets.

The refinements were carried out with a modified version of the full-matrix least-squares program of Lundgren (1979). The quantity $\sum w|F_o^2 - F_c^2|^2$ was minimized with weights $w = [\sigma^2(F_o^2) + (0{\cdot}01F_o^2)^2]^{-1}$ summing over all independent observations. Coherent neutron-scattering lengths (fm) were taken from Koester (1977). These are: 6·674 for D; 6·648 for C; 5·803 for O; and 9·579 for Cl. One scale factor and an isotropic secondary-extinction parameter (Becker & Coppens, 1974) for each data set were varied with parameters of the structural models. Extinction effects on the data were not severe, the

largest correction ($\times F_o^2$) being 1·05 (13 K) and 1·06 (100 K) for reflection 004.

Conventional refinement

The parameters varied initially included the free atomic coordinates and anisotropic thermal factors and the site-occupancy factors of D, Xe, C and Cl sites. The occupancy factors of D at convergence were found to deviate $<2\sigma$ from 0·5 and were fixed at 0·5 in final refinements. For the guest atoms, the refined values showed incomplete occupancy of the Xe site, full site occupancy of the C position within 1σ, and summed weights of the disordered Cl equal to 4·0 within 1σ. At 100 K, the occupancy and thermal factors of the disordered Cl atoms were strongly correlated ($>0{\cdot}95$), and parameter dampening was necessary to achieve convergence. In the final refinements, the variables were positional and thermal parameters and site-occupancy factors of Xe and Cl. In the final difference maps, the largest residual densities $|\rho|$, were $\sim 2\%$ of ρ at an O site and were observed in regions of the disordered Cl atoms.

CCl_4 rotator model

The refinement of the orientationally disordered CCl_4 molecule as a rigid-body was based on the formalism of Press & Hüller (1973). The nuclear-scattering density of Cl was expanded about the C position at $(\frac{3}{8}\frac{3}{8}\frac{3}{8})$ using spherical harmonics adapted* to cubic point symmetry, $\bar{4}3m$, of the molecule and lattice site. Thus, the rotational form factor of Cl in terms of the cubic harmonics, K_{lm}, is

$$F_{\rm rot}(Q) = 4\pi b \sum_l \sum_m i^l j_l(\mathbf{Q}.\mathbf{r}) C_{lm} K_{lm}(\theta,\varphi)$$

where $\mathbf{Q}$ is the scattering vector, b the Cl-scattering length, $j_l(\mathbf{Q}.\mathbf{r})$ spherical Bessel functions of order l, r the radius of the shell of Cl atoms, C_{lm} expansion coefficients of the symmetry-adapted spherical harmonics, K_{lm}, and (θ,φ) the polar angles of $\mathbf{Q}$. The adjustable parameters are the radius r and expansion coefficients C_{lm}. Program *UPALS* was modified in order to vary these parameters together with the conventional atomic parameters of D_2O, Xe and C. The four Cl atoms of CCl_4 were treated as a single scatterer centered at C with form factor $F_{\rm rot}(\mathbf{Q})$ and occupancy factor of 4. The rigid-body constraint on CCl_4 was imposed by coupling the thermal factor of the Cl scatterer to the single variable thermal factor of C allowed by site symmetry $\bar{4}3m$. The number of C_{lm} parameters is greatly restricted by symmetry, there being at most one nonzero term for each $l < 12$ and no more than two for each of the higher l orders included in these refinements. [Index selection rules for harmonic terms allowed by the crystallographic point groups are given by Kurki-Suonio (1977) and Kara & Kurki-Suonio (1981).] Contributions from Cl were found to be significant out to the data resolution $Q_{\rm max}$ of 9·8 Å^{-1}, and required a comparatively lengthy series in $F_{\rm rot}(\mathbf{Q})$ for precise evaluation. Here, the radius parameter is larger and the distribution more ordered than in other cases where spherical harmonics methods have been applied in neutron diffraction studies, for example, NH_4Br and NH_4I (Seymour & Pryor, 1970), CD_4 (Press, 1973), NaCN (Rowe, Hinks, Price, Susman & Rush, 1973), and ND_3 (Eckert, Mills & Satija, 1984). The refinements against both data sets were initiated with parameters, $r = 1{\cdot}760$ Å, $C_{00} = 1{\cdot}0$ for assumed spherically symmetric distributions of the four disordered atoms. The expansion coefficients of symmetry-allowed harmonics, increasing in order on l, were varied from initial zero values, in groups as shown in Table 3. At each stage, the listed parameters converged rapidly, in three cycles or less, and produced improved agreement for both data sets with enhanced angular modulations of the Cl density distribution. Including coefficients of orders $l = 15$, 16 for the 100 K data and $l = 18$ for 13 K data gave no improvements of fit. The final C_{lm} parameters at 100 and 13 K were taken from refinements 5 and 6, respectively, in Table 3.

Comparison of refinement results

R-factor ratio tests (Hamilton, 1965) do not provide strong criteria for choices between the two refinement procedures: for each data set, the two $wR(F^2)$ values are virtually equal and the differences in the number of variable parameters (v) are small (Table 1). χ^2 tests on parameters refined by both procedures show that the values can be accepted as taken from the same probability distribution at the 99·5% confidence level. The largest individual differences in values are $1{\cdot}2\sigma$ at 13 K and $1{\cdot}0\sigma$ at 100 K, both being in coordinates but of different atoms. For the CCl_4 molecule, the two procedures yield C—Cl bond length values which differ greatly in precision and accuracy: the C—Cl radius parameters, 1·765 (2) Å (13 K) and 1·762 (3) Å (100 K) (Table 3), are in good accord with the gas-phase R_e value of 1·766 (3) Å (Bartell, Brockway & Schwendeman, 1955); whereas, the 'discrete atom' C—Cl

* The symmetry-adapted spherical harmonics, K_{lm} ($l \le 30$), for cubic groups were generated on the CDC 7600 computer with double precision, using the recurrence formulas of Altmann & Bradley (1963). The normalized functions ($l \le 20$) were incorporated from the computer-generated file into the FORTRAN code of the crystallographic least-squares program to avoid transcription errors. These functions are identical to the one-dimensional real representations of cubic groups given by Bradley & Cracknell (1972) for $l \le 12$, except for two entries which differ by 1 in the last-listed (11th) decimal place. It should be noted that in cubic harmonics the m indices are taken as arbitrary descriptors for K_{lm} having common l indices.

Table 2. *Refinement models: space group Fd3m*

The unit-cell origin here (and Table 4) is at $\bar{3}m$, $\frac{1}{8}\frac{1}{8}\frac{1}{8}$ (*International Tables for X-ray Crystallography*, 1952) from the alternate origin, $\bar{4}3m$, used by Mak & McMullan (1965).

			Equivalent set	Site occupancy	Coordinate	Point symmetry
Host D_2O framework						
96 D atoms	in	1	192-fold(*i*)	0·5	*xyz*	1
144 D atoms		3	96-fold(*g*)	0·5	*xxz*	*m*
32 D atoms		2	32-fold(*e*)	0·5	*xxx*	3*m*
96 O atoms	in	1	96-fold(*g*)	1·0	*xxz*	*m*
32 O atoms		1	32-fold(*e*)	1·0	*xxx*	3*m*
8 O atoms			8-fold(*a*)	1·0	$\frac{1}{8}\frac{1}{8}\frac{1}{8}$	$\bar{4}3m$
Guest structure						
Xe atoms*	in		16-fold(*c*)	Refined	000	$\bar{3}m$
CCl_4 molecules (as discrete atoms)						
8 C atoms	in		8-fold(*b*)	1·0	$\frac{3}{8}\frac{3}{8}\frac{3}{8}$	$\bar{4}3m$
Cl atoms*	in	2	96-fold(*g*)	Refined	*xxz*	*m*
Cl atoms*		1	32-fold(*e*)	Refined	*xxx*	3*m*
CCl_4 molecules (as spherical rotators)						
8 C atoms	in		8-fold(*b*)	1·0	$\frac{3}{8}\frac{3}{8}\frac{3}{8}$	$\bar{4}3m$
32 Cl scatterers centered	at		8-fold(*b*)	4·0	$\frac{3}{8}\frac{3}{8}\frac{3}{8}$	$\bar{4}3m$

*Number to be determined by refinement of site-occupancy factor.

values are ~0·04 Å less by comparison and show differences of 0·02 Å (13 K) and 0·05 Å (100 K) among the three non-equivalent values. The rigid-body CCl_4 refinements clearly give the more acceptable values for the C—Cl parameter and, as seen later, the more detailed description of the configuration of CCl_4 in the host structure. The Cl nuclear densities ρ and $\sigma(\rho)$, evaluated from the final C_{lm} parameters, show no significantly non-positive values at 100 K; for the more-ordered distribution at 13 K, deviations of -2σ are observed surrounding the largest maxima, indicating effects of limited resolution of the diffraction data. The final nuclear positional and anisotropic thermal parameters obtained from refinements 6 (13 K) and 5 (100 K) of Table 3 are listed in Table 4.*

Results and discussion

The lattice periodicity and symmetry characteristic of the structure II clathrates are unchanged down to 13 K, there being a cell-volume expansion of 0·8% between 13 and 100 K. The polyhedral host D_2O structure is illustrated in Fig. 1; the crystallographically independent D_2O molecules with atomic notation are shown in Fig. 2. The individual polyhedral units, the 12-hedron and 16-hedron, are shown in Fig. 3, and their main geometric features summarized in Tables 5 and 6. Enclosures of the Xe and CCl_4 guests inside the 12-hedron and 16-hedron are illustrated in Fig. 4 with outlines of van der Waals surfaces taking radius values of Bondi (1964).

* Lists of structure factors and cubic harmonic functions K_{lm} have been deposited with the British Library Document Supply Centre as Supplementary Publication No. SUP 52481 (12 pp.). Copies may be obtained through The Technical Editor, International Union of Crystallography, 5 Abbey Square, Chester CH1 2HU, England.

The results of this study confirm the general observations that have been made concerning the structure II clathrates: the deuterium atoms occupy two sites between each hydrogen-bonded oxygen pair with equal statistical weights, and, like other guests (Davidson & Ripmeester, 1984), the CCl_4 molecule exhibits considerable rotational freedom within the water environment. The precise structure parameters reported here allow a more comprehensive description of the type II clathrates than has hitherto appeared in the literature.

The D_2O *structure*

The D_2O molecules are disordered in orientation about the oxygen vertices with deuterium atoms located in half-occupied sites, as shown in Fig. 2. Thus, the observed atomic positions and thermal vibrations are mean values averaged for the large number of different D_2O configurations possible in this structure. In this respect, the hydrogen-bonding situation in the clathrate resembles that in ice I*h*. In the clathrate, the observed dimensions of the D_2O molecules show differences that are associated both with the framework geometry and with attractive host–guest contacts, particularly within the 16-hedra (Fig. 4*b*). The O—D bond lengths and D—O—D bond angles are listed in Table 7 for the crystallographically distinct D_2O configurations. The O—D distances are in the range 0·986–1·001 Å at 13 K and show the expected systematic bond foreshortening (0·979–0·993 Å) at 100 K caused by increased thermal motion. The longest distances are found for the O*e*—D1*g* bonds that lie within close contact with Cl where CCl_4 has its orientation of highest probability. The D—O—D angles are in the range 107·9–113·7° with the largest being for D*i*—O*g*—D*i* within hexagonal faces (Fig. 3*b*). In the gas-phase D_2O

Table 3. *CCl_4 rotator refinements with symmetry-adapted spherical harmonics for site symmetry $\bar{4}3m$; values of radius and expansion coefficients C_{lm}*

Final parameters are from refinement 5 (100 K data) and refinement 6 (13 K data). The refined coefficients of symmetry-allowed harmonics $K_{15,1}$ and $K_{15,2}$ at 13 K do not differ significantly from zero.

	1		2		3		4		5		6
	13 K	100 K	13 K	100 K	13 K	100 K	13 K	100 K	13 K	100 K	13 K
$wR(F^2)$	0·178	0·125	0·135	0·086	0·071	0·045	0·052	0·042	0·042	0·039	0·040
S	5·00	3·13	3·85	2·15	2·01	1·14	1·48	1·06	1·20	0·99	1·14
Radius (Å)	1·77 (1)	1·762 (9)	1·771 (8)	1·762 (9)	1·768 (4)	1·766 (3)	1·764 (3)	1·764 (3)	1·764 (2)	1·762 (3)	1·765 (2)
C_{00}	1·00	1·00	1·00	1·00	1·00	1·00	1·00	1·00	1·00	1·00	1·00
C_{31}			−0·10 (2)	−0·130 (9)	−0·095 (8)	−0·130 (5)	−0·097 (6)	−0·131 (5)	−0·097 (5)	−0·129 (4)	−0·097 (5)
C_{41}			0·38 (3)	0·25 (2)	0·37 (1)	0·251 (8)	0·37 (1)	0·253 (8)	0·364 (8)	0·246 (8)	0·365 (8)
C_{61}			0·00 (2)	−0·00 (1)	0·014 (9)	−0·012 (6)	0·018 (7)	−0·012 (6)	0·024 (6)	−0·009 (5)	0·026 (5)
C_{71}					0·38 (2)	0·254 (9)	0·37 (1)	0·252 (9)	0·37 (1)	0·252 (8)	0·371 (9)
C_{81}					0·16 (4)	0·11 (2)	0·16 (3)	0·11 (2)	0·16 (2)	0·11 (2)	0·16 (2)
C_{91}					0·28 (2)	0·13 (1)	0·29 (2)	0·13 (1)	0·29 (1)	0·13 (1)	0·29 (1)
$C_{10,1}$					0·05 (1)	−0·02 (1)	0·06 (1)	−0·015 (9)	0·061 (8)	−0·016 (9)	0·065 (8)
$C_{11,1}$							0·21 (2)	0·11 (2)	0·19 (2)	0·11 (2)	0·20 (2)
$C_{12,1}$							−0·3 (1)	−0·2 (1)	−0·3 (1)	−0·2 (1)	−0·26 (9)
$C_{12,2}$							0·27 (2)	0·10 (2)	0·27 (1)	0·11 (1)	0·27 (1)
$C_{13,1}$									0·15 (1)	0·06 (1)	0·14 (1)
$C_{14,1}$									0·10 (2)	0·06 (2)	0·10 (1)
$C_{16,1}$											0·15 (6)
$C_{16,2}$											0·14 (3)
$C_{17,1}$											0·14 (5)

Table 4. *Atomic positions ($\times 10^5$) and thermal parameters ($\times 10^4$)*

Parameters at 13 and 100 K are given on first and second lines, respectively. Thermal factors have the form: $\exp[-2\pi a^{*2}(h^2U_{11} + k^2U_{22} + l^2U_{33} + 2hkU_{12} + 2hlU_{13} + 2klU_{23})]$. Estimated standard deviations given in parentheses refer to last significant digits; where none is given the parameters are either fixed or constrained by symmetry, except as noted below.

	Occupancy	x	y	z	U_{11}	U_{22}	U_{33}	U_{12}	U_{13}	U_{23}
D*i*	0·50	−16179 (7)	−2043 (6)	14456 (7)	270 (6)	226 (5)	234 (5)	−82 (4)	15 (4)	−74 (4)
	0·50	−16185 (7)	−2058 (6)	14416 (7)	334 (6)	281 (5)	309 (6)	−66 (4)	12 (4)	−71 (4)
D3*g*	0·50	14153 (5)	14153	37149 (10)	223 (4)	223	224 (7)	4 (5)	−10 (4)	−10
	0·50	14199 (6)	14199	37082 (11)	273 (5)	273	314 (8)	−8 (6)	−11 (4)	−11
D2*g*	0·50	19523 (7)	19523	31480 (10)	255 (5)	255	146 (7)	34 (6)	2 (4)	2
	0·50	19487 (8)	19487	31499 (11)	314 (6)	314	230 (8)	27 (7)	16 (5)	16
D1*g*	0·50	20464 (7)	20464	27236 (10)	248 (5)	248	173 (8)	6 (6)	5 (4)	5
	0·50	20493 (7)	20493	27178 (11)	298 (5)	298	258 (8)	−2 (6)	12 (4)	12
D2*e*	0·50	15830 (11)	15830	15830	198 (5)	198	198	−24 (6)	−24	−24
	0·50	15794 (11)	15794	15794	270 (6)	270	270	−45 (7)	−45	−45
D1*e*	0·50	18337 (10)	18337	18337	201 (5)	201	201	−36 (7)	−36	−36
	0·50	18352 (11)	18352	18352	262 (6)	262	262	−24 (8)	−24	−24
O*g*	1·00	18219 (3)	18219	36956 (5)	143 (2)	143	112 (3)	46 (3)	−25 (2)	−25
	1·00	18215 (3)	18215	36943 (5)	215 (3)	215	192 (4)	29 (3)	−16 (2)	−16
O*e*	1·00	21671 (5)	21671	21671	127 (2)	127	127	−10 (3)	−10	−10
	1·00	21658 (5)	21658	21658	200 (3)	200	200	0 (3)	0	0
O*a*	1·00	12500	12500	12500	102 (5)	102	102	0	0	0
	1·00	12500	12500	12500	179 (6)	179	179	0	0	0
C	1·00	37500	37500	37500	76 (1)	76	76	0	0	0
	1·00	37500	37500	37500	146 (1)	146	146	0	0	0
Cl	4·00	37500	37500	37500	76†	76	76	0	0	0
	4·00	37500	37500	37500	146†	146	146	0	0	0
Xe	0·22 (1)	00000	00000	00000	180 (30)	180	180	0	0	0
	0·21 (1)	00000	00000	00000	311 (40)	311	311	0	0	0

†Thermal factor U_{ii} of Cl distribution is coupled to variable U_{11} of C atom in refinements.

molecule in ground vibrational state, the average O—D distance and D—O—D angle are 0·9687 Å and 104·35° (Cook, DeLucia & Helminger, 1974).

It is observed in general that there is a strengthening of hydrogen bonding in going from a water dimer to two- or three-dimensional water structures. This 'cooperative effect' in structured water is understood to mean that the geometric and energetic aspects of hydrogen-bonding display non-additive characteristics when a water molecule serves as both a hydrogen-bond donor and acceptor (Newton, 1986, and references therein). It is well known that the O—D distance is one parameter which increases with hydrogen-bond strength and thus can be used to ascertain the effect of cooperative bonding on the molecular dimensions of water in various configurations. In the clathrate structure, the O—D distances increase between 0·010 and 0·033 Å (13 K) as compared with the O—D gas-phase value of 0·9687 Å (Cook *et al.*, 1974). *Ab initio* calculations of water clusters (Newton, 1986) predict bond-length increases of from 0·005 Å in the H_2O dimer and up to 0·02 Å in ice I*h* in good agreement with the above observations. A further lengthening of 0·01 Å is observed in the O*e*—D1*g* bonds that are associated with close contact with Cl atoms of CCl_4. It is also of

interest to compare the experimental bonding parameters of water in this framework with values in the linear chains of the zeolite, bikitaite, also derived from 13 K single-crystal neutron diffraction data (Ståhl, Kvick & Ghose, 1989). In the bikitaite structure, the hydrogen-bonded O—H distances of 0·969 (3) and 0·972 (3) Å are marginally longer than the non-hydrogen-bonded distances of 0·960 (3) and 0·961 (3) Å for H_2O molecules in the chain. Thus, hydrogen bonds in the linear chain are weaker than in the three-dimensional arrangement in the clathrate crystal.

The hydrogen-bond distances and angles in the clathrate framework are listed in Table 8. The O···O distances vary between 2·731 (1) and 2·785 (1) Å at 13 K and are increased [2·735 (2)–2·795 (1) Å] at 100 K; the corresponding O···D distances are 1·739 (4)–1·802 (1) and 1·751 (4)–1·813 (1) Å, respectively. The angles O—D···O are all almost linear and fall in the range 174·8 (1)–180·0° (13 K) [175·0 (1)–180·0° (100 K)]. The shorter and stronger O···D hydrogen bonds involve D_2O configurations of oxygen O*e*, consistent with the above observations on the O—D bond lengthening. The somewhat stronger hydrogen-bond interaction here, as compared to the situation in ice I*h* (Kuhs & Lehmann, 1987) may be attributed to the interaction of the host water with guest molecules causing further polarization of the electrons in the hydrogen-bond acceptor and donor atoms.

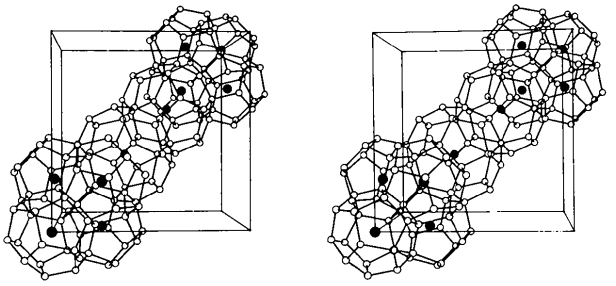

Fig. 1. Stereogram illustrating the characteristic packing of oxygen polyhedra in the cubic II framework with two 16-hedra centered at $(\frac{3}{8},\frac{3}{8},\frac{3}{8})$ and $(\frac{5}{8},\frac{5}{8},\frac{5}{8})$, and two clusters of four 12-hedra centered at $(\frac{1}{8},\frac{1}{8},\frac{1}{8})$ and $(\frac{7}{8},\frac{7}{8},\frac{7}{8})$ in a view down the *a* axis. The solid circles represent Xe and C atoms inside the 12-hedra and 16-hedra, respectively.

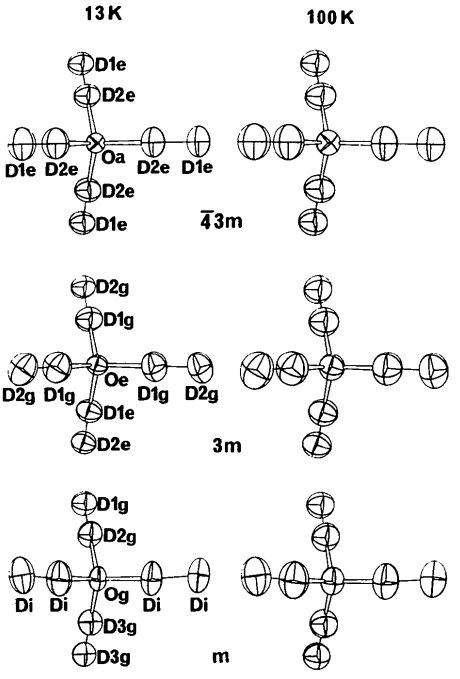

Fig. 2. Configurations of the three unique D_2O molecules showing the D atoms in positions of twofold disorder. Ellipsoid surfaces are at 50% probability level (Johnson, 1976). Dimensions in Table 7 are derived from mean nuclear positions and are subject to effects of (1) displacive disorder of D_2O molecules in different hydrogen-bonding environments, (2) librational motion and (3) internal vibrations.

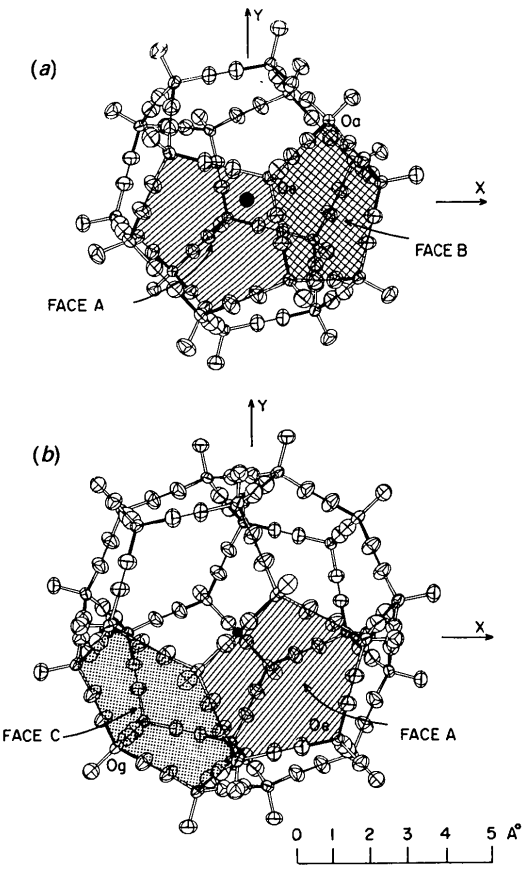

Fig. 3. The dodecahedron of $(D_2O)_{20}$ (*a*) and hexakaidecahedron of $(D_2O)_{28}$ (*b*), with D atoms shown in disordered positions. Ellipsoids as in Fig. 2; those of Xe in (*a*) and C in (*b*) are darkened for constrast (13 K data).

The clathrate guest enclosures

Xenon. The refined Xe parameters (Table 4) show statistical occupancy of 22 (1)% of the 12-hedra cavities, in good agreement with the value of 20% obtained in crystal-growth studies (Waller, 1960). The geometry of enclosure is well illustrated in Fig. 4(*a*). The Xe···O and Xe···D distances are in the ranges 3·52–3·75 and 3·72–3·92 Å (13 K), respectively, the shortest being between Xe and D_2O*a*. These exceed the sums of van der Waals radii (Bondi, 1964) by 0·16–0·39 Å for both Xe···O and Xe···D. The shorter free-distance values are comparable with the $\langle u^2\rangle^{1/2}$ components of atomic vibrational amplitudes (0·137 Å for Xe, 0·152 Å for D, 0·106 Å for O) that are evaluated in Xe···D and Xe···O directions from the 13 K U_{ij} thermal parameters.

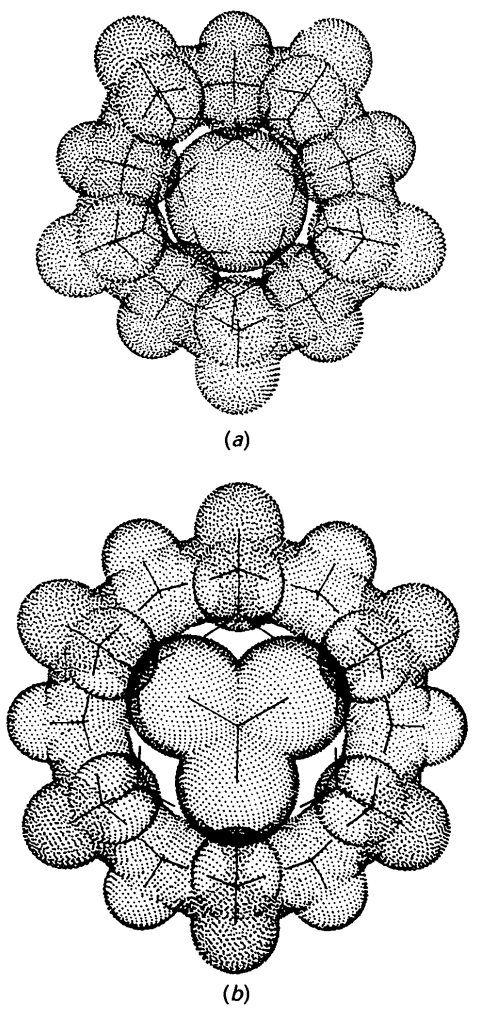

Fig. 4. Van der Waals surfaces representing enclosures of Xe in 12-hedron (*a*) and CCl_4 in 16-hedron (*b*), in views normal to pentagonal and hexagonal faces, respectively. Atoms of the upper and lower faces of the two cages are omitted for clarity. The CCl_4 molecule is illustrated in one of its three 'equilibrium' orientations, *cf.* Fig. 5. Radius values: 1·2 Å for D; 1·4 Å for O; 1·75 Å for Cl; 2·16 Å for Xe (Bondi, 1964).

Table 5. *Dimensions* (Å) *of polyhedra*

	Dodecahedron	Hexakaidecahedron
Center	(0,0,0)	$(\frac{3}{8},\frac{3}{8},\frac{3}{8})$
Faces	6(*A*) + 6(*B*)	12(*A*) + 4(*C*)
Vertices	2(O*a*) + 6(O*e*) + 12(O*g*)	4(O*e*) + 24(O*g*)
Center–vertices	3·72–3·92	4·61–4·71
Center–face(centers)		
A	3·13	4·00
B	3·04	—
C	—	3·72
Vertex–face(centers)		
A	2·30–2·40	2·30–2·40
B	2·32–2·35	—
C	—	2·39

Table 6. *Distances* (Å) *from least-squares planes defined by oxygen atoms*

Face *A*

Oe	2Og	2Og	2D1g	2D2g	2D3g	2D*i*	2D*i*
−0·018	+0·015	−0·005	+0·003	+0·016	+0·025	+0·046	+0·055
−0·019	+0·015	−0·006	+0·009	+0·012	+0·016	+0·046	+0·055

Average e.s.d. from plane: O 0·002, D 0·002 at 13 K; O 0·004, D 0·004 at 100 K

Face *B*

Planar by symmetry

Face *C*

3Og	3Og	3D*i*	3D*i*
+0·052	−0·052	+0·032	−0·032
+0·051	−0·051	+0·029	−0·029

Average e.s.d. from plane: O 0·003, D 0·002 at 13 K; O 0·005, D 0·004 at 100 K

Carbon tetrachloride. The enclosure of the CCl_4 molecule in the 16-hedra (Fig. 4*b*) leads to Cl···O and Cl···D contact distances as much as 0·2 Å less than sums of the van der Waals radii. The center-of-mass displacements, $\langle u^2\rangle^{1/2}$, from the carbon U_{ii} parameters are 0·087 Å (13 K) and 0·121 Å (100 K), compared with the average oxygen displacements $\langle u^2\rangle^{1/2}$ of 0·113 Å (13 K) and 0·144 Å (100 K). In Fig. 5, the orientation-averaged scattering densities of Cl at 13 and 100 K are mapped on spherical surfaces using the final C_{lm} parameter values in Table 3. At 13 and 100 K, the major features are similar in their distributions on the surface; those at 13 K show enhanced density expected for increased rotational order between 13 and 100 K. The centroids of maximum density define three distinct 'equilibrium' CCl_4 orientations in which the C→Cl vectors point approximately toward the cage oxygen atoms (*cf.* Fig. 5.). Orientations labelled α, β, γ, in Figs. 5 and 6, are associated with cage D_2O configurations of 2O*g* and O*e*, respectively, (Fig. 7). In the γ orientation, the C→Cl vectors are coincident with the crystallographic [111] direction, and the T_d symmetry of the molecule is fully utilized. In the less well defined α and β orientations, the C→Cl vectors are in directions of oxygen vertices O*g* of the four hexagonal faces *C* (Fig. 3*b*). In these orientations, no sets

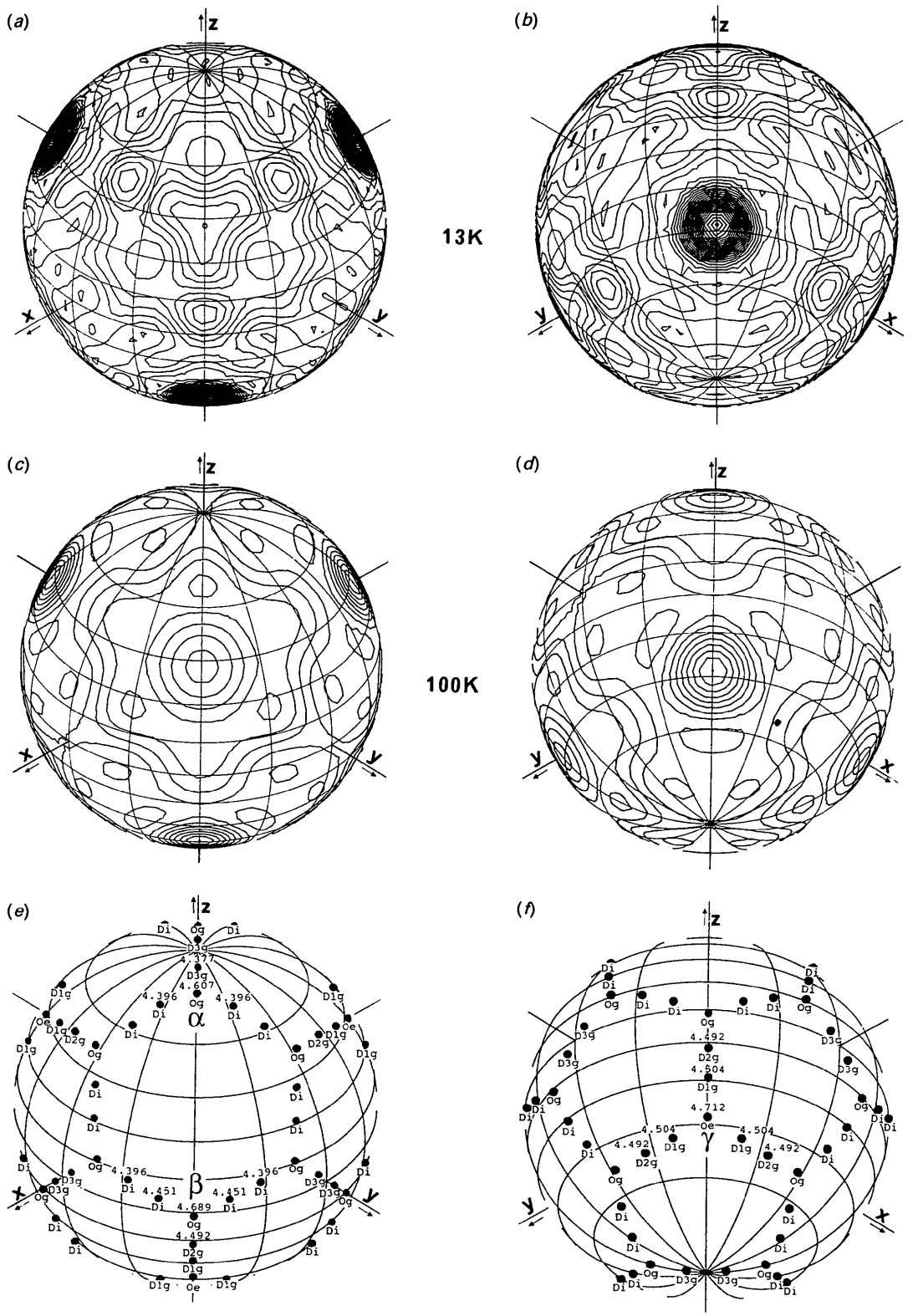

Fig. 5. Scattering density of four Cl atoms on the surface of a sphere, evaluated from the function $G(\theta,\varphi) = 4\pi\Sigma_l\Sigma_m C_{lm}K_{lm}(\theta,\varphi)$ with coefficients C_{lm} of the cubic harmonics, K_{lm}, derived from refinement. Views are along the [111] direction: with (*a*) and (*c*) towards the origin, and (*b*) and (*d*) away from the origin. Views (*e*) and (*f*) show poles of C→O and C→D vectors on the surface with distances (Å) from the cage center. Labels α, β, γ indentify the three distinct CCl_4 orientations not related by symmetry $\bar{4}3m$.

Table 7. *Bond lengths* (Å) *and angles* (°) *in water molecules*

Values at 13 and 100 K appear on the first and second lines, respectively.

	Configuration						
	D*i*—O*g*—D*i*	D3*g*—O*g*—D*i*	D2*g*—O*g*—D*i*	D3*g*—O*g*—D2*g*	D1*g*—O*e*—D1*g*	D1*e*—O*e*—D1*g*	D2*e*—O*a*—D2*e*
Number*	1	2	2	1	3	3	6
D—O†	0·986 (1)	0·989 (2)	0·993 (2)		1·001 (2)	0·992 (3)	0·991 (3)
	0·984 (1)	0·979 (2)	0·988 (2)		0·993 (2)	0·987 (4)	0·984 (3)
D—O—D	113·5 (1)	108·5 (1)	107·9 (1)	110·5 (2)	110·7 (1)	108·2 (1)	109·47
	113·7 (1)	108·9 (1)	107·8 (1)	109·7 (2)	110·3 (1)	108·6 (1)	109·47

* Number of crystallographically equivalent configurations defined by D positions in Fig. 2.
† Refers to first listed D—O distance of configuration.

Table 8. *Hydrogen-bond distances* (Å) *and angles* (°)

Values at 13 and 100 K appear on the first and second lines, respectively.

	O*g*—D*i*···O*g*	O*g*—D3*g*···O*g*	O*g*—D2*g*···O*e*	O*e*—D1*g*···O*g*	O*a*—D2*e*···O*e*	O*e*—D1*e*···O*a*
O—D	0·986 (1)	0·989 (2)	0·993 (2)	1·001 (2)	0·992 (3)	0·993 (3)
	0·984 (1)	0·979 (2)	0·988 (2)	0·993 (2)	0·984 (3)	0·987 (4)
O···D	1·802 (1)	1·793 (2)	1·765 (2)	1·758 (2)	1·739 (4)	1·738 (3)
	1·813 (1)	1·808 (2)	1·777 (2)	1·773 (2)	1·751 (4)	1·748 (3)
O—D···O	174·8 (1)	177·0 (2)	178·6 (3)	179·0 (3)	180·0	180·0
	175·0 (1)	177·8 (2)	179·0 (2)	178·4 (2)	180·0	180·0
O···O	2·785 (1)	2·781 (2)	2·759 (1)		2·731 (1)	
	2·795 (1)	2·787 (2)	2·766 (1)		2·735 (2)	
	13 K	100 K		13 K	100 K	
O*g*···O*g*···O*g*	119·86 (3)	119·87 (3)	O*g*···O*e*···O*a*	107·55 (3)	107·59 (4)	
O*g*···O*g*···O*g*	108·58 (3)	108·56 (3)	O*g*···O*e*···O*g*	111·32 (3)	111·28 (3)	
O*e*···O*g*···O*g*	105·75 (3)	105·78 (4)	O*e*···O*a*···O*e*	109·47	109·47	
O*e*···O*g*···O*g*	107·71 (3)	107·67 (4)				

of four O*g* positions subtend angles at the cage center which closely fit the angles of CCl_4, and dispersion of Cl density for orientations α and β is an expected consequence. Moreover, since the two oxygen O*g* configurations (Fig. 7) occupy similar geometric positions in the cage, the CCl_4 molecule appears to populate orientations α and β with similar densities as seen in Figs. 5 and 6. It should be noted that surface-density minima, and low probability of orientations, are observed where the C→Cl vectors are directed toward centers of the hexagonal and pentagonal faces.

Between 100 and 13 K, there is a remarkable increased density observed for the γ orientation with only marginal density increases for orientations α and β, indicating that the observed ordering of CCl_4 occurs from free rotation or orientations other than α and β. Moreover, the angular dispersion of density from orientations α, β, γ appears to be temperature independent. For the more clearly defined γ orientation, the density is approximately Gaussian with full-widths at half-heights of ~20° (13 K) and 25°

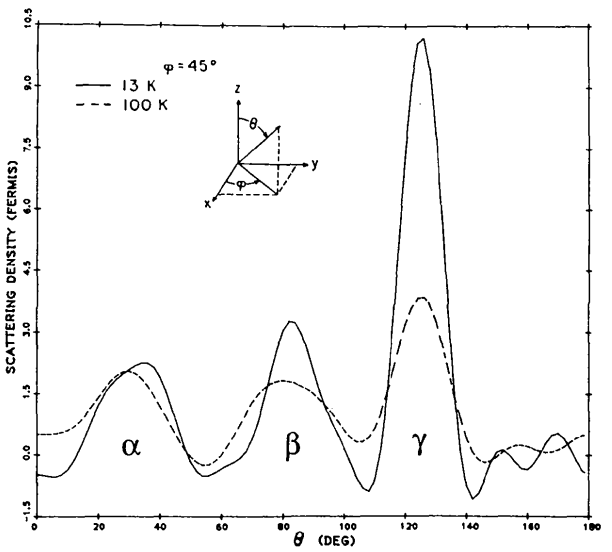

Fig. 6. Traces of the Cl-scattering density between $\pm z$, at $x = y$ ($\varphi = 45°$). Labels α, β, γ are as in Fig. 5.

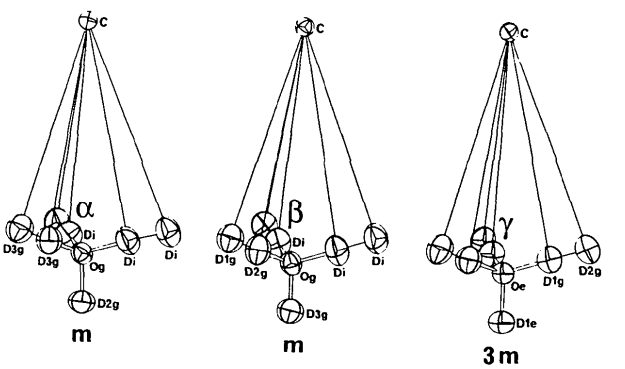

Fig. 7. The three D_2O molecules of the 16-hedron not related by $\bar{4}3m$ symmetry. The cone angles, D···C···D, subtended at C are ~10 and ~20° for D—O—D and D···O···D configurations, respectively.

(100 K), which correspond to twice the cone angle subtended at the cage center by the O—D bond length. Thus, it is inferred that the C→Cl vectors are not pointing toward the oxygen vertices, but rather are 'precessing' around these directions coupled to deuteron disorder in molecules $(D_2O)e$ and $(D_2O)g$ by weak attractive interactions.

We are grateful to Mr Joseph Henriques for technical assistance, to Dr Christopher Ashton for use of his computer programs in illustrating spherical harmonics functions, and to Dr Enrique Abola for his help with other computer-graphics displays.

References

ALTMANN, S. L. & BRADLEY, C. J. (1963). *Philos Trans. R. Soc. London Ser. A*, **255**, 193–198.

BARTELL, L. S., BROCKWAY, L. O. & SCHWENDEMAN, R. H. (1955). *J. Chem. Phys.* **23**, 1854–1859.

BECKER, P. J. & COPPENS, P. (1974). *Acta Cryst.* A**30**, 129–147.

BONDI, A. J. (1964). *J. Phys. Chem.* **68**, 441–451.

BRADLEY, C. J. & CRACKNELL, A. P. (1972). *The Mathematical Theory of Symmetry in Solids*, ch. 2. Oxford: Clarendon Press.

COOK, R. L., DELUCIA, F. C. & HELMINGER, P. (1974). *J. Mol. Spectrosc.* **53**, 62–76.

DAVIDSON, D. W. & RIPMEESTER, J. A. (1984). *Inclusion Compounds*, Vol. 3, edited by J. L. ATWOOD, J. E. D. DAVIES & D. D. MACNICOL, pp. 69–128. London: Academic Press.

ECKERT, J., MILLS, R. L. & SATIJA, S. K. (1984). *J. Chem. Phys.* **81**, 6034–6038.

HAMILTON, W. C. (1965). *Acta Cryst.* **18**, 502–510.

HUTCHINGS, M. T., SCHULHOF, M. P. & GUGGENHEIM, H. J. (1972). *Phys. Rev. B*, **5**, 154–168.

International Tables for X-ray Crystallography (1952). Vol. I. Birmingham: Kynoch Press.

International Tables for X-ray Crystallography (1962). Vol. III. Birmingham: Kynoch Press. (Present distributor Kluwer Academic Publishers, Dordrecht.)

JEFFREY, G. A. (1984). *Inclusion Compounds*, Vol. 1, edited by J. L. ATWOOD, J. E. D. DAVIES & D. D. MACNICOL, pp. 135–190. London: Academic Press.

JOHNSON, C. K. (1976). *ORTEP*II. Report ORNL-5138. Oak Ridge National Laboratory, Tennessee, USA.

KARA, M. & KURKI-SUONIO, K. (1981). *Acta Cryst.* A**37**, 201–210.

KOESTER, L. (1977). *Springer Tracts in Modern Physics, Neutron Physics*, edited by G. HÖHLER, pp. 36–38. Berlin: Springer.

KUHS, W. F. & LEHMANN, M. S. (1987). *J. Phys. (Paris) Colloq. C1*, **48**, 3–8.

KURKI-SUONIO, K. (1977). *Isr. J. Chem.* **16**, 115–123.

LUNDGREN, J.-O. (1979). Report UUICB13-4-03. Institute of Chemistry, Univ. of Uppsala, Sweden.

MAK, T. C. W. & MCMULLAN, R. K. (1965). *J. Chem. Phys.* **42**, 2732–2737.

MEULENAER, J. DE & TOMPA, H. (1965). *Acta Cryst.* **19**, 1014–1018.

NEWTON, M. D. (1986). *Trans. Am. Crystallogr. Assoc.* **22**, 1–17.

PRESS, W. (1973). *Acta Cryst.* A**29**, 257–263.

PRESS, W. & HÜLLER, A. (1973). *Acta Cryst.* A**29**, 252–256.

ROWE, J. M., HINKS, D. G., PRICE, D. L., SUSMAN, S. & RUSH, J. J. (1973). *J. Chem. Phys.* **58**, 2039–2042.

SEYMOUR, R. S. & PRYOR, A. W. (1970). *Acta Cryst.* B**26**, 1487–1491.

STACKELBERG, M. VON & FRÜHBUSS, H. (1954). *Z. Elektrochem.* **58**, 99–104.

STACKELBERG, M. VON & MÜLLER, H. R. (1954). *Z. Elektrochem.* **58**, 25–39.

STÅHL, K., KVICK, Å. & GHOSE, S. (1989). *Zeolites*. In the press.

TEMPLETON, L. K. & TEMPLETON, D. H. (1973). Abstr. Am. Crystallogr. Assoc. Meet., Storrs, Connecticut p. 143.

WALLER, J. G. (1960). *Nature (London)*, **186**, 429–431.

Acta Cryst. (1990). B**46**, 399–405

Crystal and Molecular Structures of the Inclusion Compounds of Cholic Acid with Methanol, Ethanol and 1-Propanol

BY ELIZABETH L. JONES AND LUIGI R. NASSIMBENI*

Department of Chemistry, Univeristy of Cape Town, Rondesbosch 7700, *South Africa*

(*Received* 24 *August* 1989; *accepted* 20 *December* 1989)

Abstract

The 1:1 inclusion compounds of cholic acid with methanol ($C_{24}H_{40}O_5.CH_4O$), ethanol ($C_{24}H_{40}O_5.C_2H_6O$) and 1-propanol ($C_{24}H_{40}O_5.C_3H_8O$) crystallize in the $P2_12_12_1$ space group with unit-cell dimensions at 293 K: $a = 15{\cdot}198$ (6), $b = 11{\cdot}625$ (7), $c = 14{\cdot}560$ (9) Å; $a = 14{\cdot}653$ (7), $b = 11{\cdot}739$ (4), $c = 15{\cdot}045$ (2) Å; and $a = 15{\cdot}026$ (2), $b = 11{\cdot}864$ (9), $c = 14{\cdot}951$ (4) Å; $Z = 4$. The structures were solved using direct methods. Full-matrix least-squares refinement reduced the conventional R factor to values of 0·109, 0·066 and 0·071, respectively. The alcohol molecules are contained in cavities created by the cholic acid molecules and are involved in the hydrogen-bonding scheme consisting of five unique hydrogen bonds. Statistical disorder is observed for the ethanol and 1-propanol molecules.

Introduction

The bile acids are derivatives of the steroid 5β-cholan-24-oic acid. *In vivo*, the bile acids are conjugated with the amino acids glycine and taurine and exist as salts of sodium or potassium in the bile.

* To whom correspondence should be addressed.

0108-7681/90/030399-07$03.00